

Probing the ν Mass Hierarchy via Atmospheric $\nu_\mu + \bar{\nu}_\mu$ Survival Rates in Megaton Water Čerenkov Detectors

Raj Gandhi ^{a,*}, Pomita Ghoshal ^{a,†}, Srubabati Goswami ^{a,‡}, Poonam Mehta ^{a,b,§},
S Uma Sankar ^{c,¶}

^a*Harish-Chandra Research Institute, Chhatnag Road, Jhansi,
Allahabad 211 019, India*

^b*Department of Particle Physics, Weizmann Institute of Science,
Rehovot 76 100, Israel*

^c*Department of Physics, Indian Institute of Technology, Powai,
Mumbai 400 076, India*

Abstract

The neutrino mass hierarchy, presently unknown, is a powerful discriminator among various classes of unification theories. We show that the $\nu_\mu + \bar{\nu}_\mu$ survival rate in atmospheric events can provide a novel method of determining the hierarchy in megaton water Čerenkov detectors. For pathlength and energy ranges relevant to atmospheric neutrinos, this rate obtains significant matter sensitive variations not only from resonant matter effects in $P_{\mu e}$ but also from those in $P_{\mu\tau}$. We calculate the expected muon event rates in the case of matter oscillations with both natural and inverted hierarchy. We identify the energy and pathlength ranges for which resonant matter effects can lead to observable differences between the above two cases. We also estimate the exposure time required to observe this difference and determine the sign of Δ_{31} in a statistically significant manner.

*Email: raj@mri.ernet.in

†Email: pomita@mri.ernet.in

‡Email: sruba@mri.ernet.in

§Email: mpoonam@mri.ernet.in, poonam@wisemail.weizmann.ac.il

¶Email: uma@phy.iitb.ac.in

1 Introduction

An oft-repeated statement is that the recent evidence for neutrino mass and oscillations [1] constitutes proof of physics beyond the Standard Model. The important sub-text to this, however, is that the nature of this physics remains, at present, largely unknown, with very many possibilities and open questions. The quest for this new physics is closely linked to several unknowns in the neutrino sector :

- (a) The absolute scale of neutrino masses,
- (b) The hierarchy of neutrino masses,
- (c) The magnitude of the lepton mixing matrix element U_{e3} (see below),
- (d) The value of the leptonic CP violating phase δ_{CP} , and
- (e) The Dirac or Majorana nature of neutrinos.

The *hierarchy of neutrino masses* m_i , ((b) above) with $i = 1, 2, 3$, refers to the ordering of the mass eigenstates. Given the fact that $\Delta_{21} = m_2^2 - m_1^2 > 0$ from solar neutrino data, knowing the hierarchy translates to determining the (as yet unknown¹) sign of $\Delta_{31} = m_3^2 - m_1^2$, henceforth referred to as $\text{sign}(\Delta_{31})$. Specifically, if this sign is positive, (*i.e.* $m_3^2 > m_2^2 > m_1^2$) the hierarchy is termed *normal* (NH), and if it is negative (*i.e.* $m_2^2 > m_1^2 > m_3^2$), the hierarchy is said to be *inverted* (IH). The neutrino mixing matrix U , with elements $U_{\alpha i}$ relating the flavour or weak interaction eigenstates (labeled by $\alpha = e, \mu, \tau$) to the mass eigenstates (labeled by $i = 1, 2, 3$) leads to the same flavour composition for a given mass state whether the hierarchy is normal or inverted. Attempts to construct a unified theory beyond the Standard Model however, depend crucially on $\text{sign}(\Delta_{31})$; in fact, one way to classify families of models is via the neutrino hierarchy they assume as input.

A large class of Grand Unified Theories (GUTs) use the Type I seesaw mechanism [2], requiring the existence of heavy right-handed neutrinos at the GUT scale to generate small neutrino masses. Since GUTs typically unify quarks and leptons, and the quark hierarchy is normal, such models favour a normal neutrino hierarchy. Typically, if one uses an inverted hierarchy to construct a Type I seesaw model, one finds [3] that the light neutrino mass spectrum may become very sensitive to small changes in the heavy neutrino masses and to radiative corrections. Inverted hierarchies imply the near degeneracy of the states m_2 and m_1 , and since a corresponding degeneracy is absent in the quark sector, they may require the presence of an additional global symmetry in the lepton sector. Additionally, important features of leptogenesis, which may help partially understand the present matter-antimatter asymmetry of the universe, are significantly different in the two cases. In general, GUTs based on Type I seesaw models strongly depend on a normal mass hierarchy to obtain their many desirable features[3]. An inverted hierarchy, on the other hand, would favour the possibility of a unified theory based on a Type II seesaw mechanism, employing additional Higgs triplets,

¹Our knowledge of $\Delta_{31} = m_3^2 - m_1^2$ derives from atmospheric and long baseline accelerator (K2K) data, which are sensitive only to its magnitude.

or on models which require a (global) lepton flavour symmetry. The hierarchy is thus a crucial marker in our quest for a unified theory, and its determination would be helpful in eliminating or at the very least strongly disfavours large classes of such theories and in considerably narrowing the focus of this search.

Generally speaking, determination of the mass hierarchy requires the observation of resonant matter effects (*i.e.* long baselines) and a not too small $\sin^2 2\theta_{13} (\gtrsim 0.05)^2$. Among the next generation long baseline accelerator experiments, combined results from T2K [5, 6] and the NuMI Off-axis experiment NO ν A [7] may be able to infer the neutrino mass hierarchy [8, 9, 10, 11]. It is also possible to determine the hierarchy in experiments using beta beams [12] and neutrino factories [13]. However these experiments use the $\nu_\mu \leftrightarrow \nu_e$ channel, the sensitivity of which is compromised by the ambiguities resulting from inherent degeneracies. Specifically, these originate in inter-relations between the $\text{sign}(\Delta_{31})$, the phase δ_{CP} and the mixing angle θ_{13} [14]. To overcome this, the synergistic use of two experiments, sometimes with more than one measurement each will be necessary [15, 16, 17, 18, 19, 20]. Alternatively, two detectors at different distances [21, 22] have been suggested. For baselines contemplated for the next generation of accelerator and superbeam experiments (*i.e.* $\lesssim 800$ km), much of the decrease in sensitivity arises from the δ_{CP} - $\text{sign}(\Delta_{31})$ degeneracy. Its effect tends to decrease for much longer baselines, vanishing, in fact, for the magic baseline where the δ_{CP} terms go to zero [23, 24, 25]. The use of earth matter effects in atmospheric muon neutrinos for the determination of the hierarchy has been studied in the context of magnetized iron calorimeter detectors in [26, 27, 28] and water Čerenkov detectors in [29]. In particular, it was shown in [28] that the effect of degeneracies are not significant in the muon survival probability for the large baselines involved. Matter effects in supernova neutrinos can also, in principle, determine the neutrino mass hierarchy [30]. However large uncertainties in supernova neutrino fluxes reduce the sensitivity. Finally, if neutrinos are Majorana particles then determination of mass hierarchy may be possible from next generation neutrino-less double beta experiments [31], provided hadronic uncertainties in the nuclear matrix elements are reduced from their present levels. Non-oscillation probes of the neutrino mass hierarchy and the limit of small $\sin^2 2\theta_{13}$ have been discussed recently in [32].

Megaton water Čerenkov detectors constitute an important future class of detectors with significant capabilities. The projects under active consideration are UNO [33] in the US, a megaton detector in the Frejus laboratory [34] in Europe, and the HyperKamiokande (HK) project [6, 35] in Japan. Such massive detectors would enable impressive measurements of atmospheric neutrino parameters. Specifically, they would determine $|\Delta_{31}|$ and $\sin^2 \theta_{23}$ to the few percent level, and obtain a much improved bound on θ_{13} . Since the water Čerenkov technique is not sensitive to the charge of the produced lepton on an event by event basis, the combined signal for neutrinos and antineutrinos must be searched for using statistical discriminators in order to determine the mass hierarchy. At present, the method which is contemplated for discriminating between neutrino and antineutrino interactions involves using the differences in the total cross section σ and its rapidity³ dependence ($d\sigma/dy$). Neutrino-nucleon interactions in the few GeV to 10 GeV range have a higher average rapidity than the corresponding

²While these conditions are sufficient, they are not necessary. If they are not satisfied, however, qualitatively different experimental approaches entailing a significantly higher degree of precision will be required [4].

³Rapidity is defined as $y = (E_\nu - E_{\text{lepton}})/E_\nu$.

antineutrino-nucleon interactions, and thus produce more multi-hadron events. Thus an enhanced signal for multi-ring electron-like events is expected in water Čerenkov detectors if the hierarchy is normal than if it is inverted [29, 35]. Given the importance of the hierarchy to theoretical efforts towards unification, it is recommended that we explore multiple approaches to this problem. In this paper, we exploit the sensitivity of the muon survival rate to *resonant* matter effects (as opposed to merely matter *enhanced* effects) for detecting the hierarchy in megaton Čerenkov detectors. Our method consists of a careful selection of energy and zenith angle bins for which the resonant matter effect in muon neutrino survival probability is observationally significant. We perform realistic event-rate calculations for atmospheric muon rates in such detectors, which incorporate their efficiencies and lie within their resolutions. We show that for $\sin^2 2\theta_{13} = 0.1$ and \sim a 3 year run, signals with statistical significance in excess of 4σ are possible for pathlength and energy ranges where the muon survival probability is matter sensitive. As mentioned above, the results are largely free of parameter degeneracies and associated ambiguities.

2 Earth - matter effects in $P_{\mu\mu}$

As is well known the matter effects in neutrino oscillations arise due to the difference in the interactions of ν_μ/ν_τ and ν_e as they traverse matter [36]. The mixing angle θ_{13} parameterizes the admixture of ν_e with ν_μ/ν_τ in the oscillations driven by the larger mass-square difference Δ_{31} . Hence all matter effects in oscillations, such as those which manifest themselves in long baseline and atmospheric neutrino experiments, are proportional to sine of this angle. The CHOOZ experiment constrains $\sin^2 2\theta_{13}$ to be ≤ 0.2 [37]. For the energy which satisfies the resonance condition [38]

$$\Delta_{31} \cos 2\theta_{13} = 0.76 \times 10^{-4} \rho(\text{gm/cc}) E(\text{GeV}) \quad (1)$$

the matter dependent θ_{13} gets amplified to $\pi/4$ and matter effects lead to large changes in the survival/oscillation probabilities, provided the pathlength dependent oscillating term is also close to 1.

Resonant matter effects involving $\nu_\mu \rightarrow \nu_e$ transitions have been extensively studied in the literature [39]. Most studies of next generation accelerator neutrino experiments, seeking to probe the mass hierarchy seek to exploit the matter effects in $P_{\mu e}$. These experiments have baselines ranging from 300 km to 3000 km and energies in the \sim GeV range. For such ‘short’ baselines and for energies in the few GeV range, while the percentage change in $P_{\mu e}$ can be large, its absolute value remains modestly small, since *resonant* matter effects do not develop. However, for the baseline range 6000 - 10500 km, since $\sin^2 2\theta_{13}^m$ then gradually builds to ~ 1 , $P_{\mu\mu}$ and $P_{\mu\tau}$ exhibit large matter sensitive variations, especially if resonance occurs in the neighbourhood of a vacuum peak. In such a situation, the oscillating factors in the survival/oscillation probabilities are large. This in turn synergistically converts a large change in $\sin^2 2\theta_{13}$ due to matter effects into a large change in survival/oscillation probabilities.

It is difficult to observe the *resonant* amplification of the matter effects in $\nu_\mu \rightarrow \nu_e$ oscillations, because the pathlength for which this occurs is inversely proportional to $\tan 2\theta_{13}$. For

almost all allowed values of θ_{13} , except those near the current upper bound, this pathlength is close to or larger than the diameter of earth [40]:

$$[\rho L]_{\mu e}^{\max} \simeq \frac{(2p+1)\pi \times 10^4}{2 \tan 2\theta_{13}} \text{ km gm/cc}, \quad (2)$$

where ρ is the average density of the earth along the path and p is a positive integer ≥ 0 . However, the pathlength for which resonant matter effects in $P_{\mu\mu}$ are maximum is given by [40]

$$[\rho L]_{\mu\mu}^{\max} \simeq p\pi \cos 2\theta_{13} \times 10^4 \text{ km gm/cc}, \quad (3)$$

where p is a positive integer > 0 . For all allowed values of θ_{13} , $\cos 2\theta_{13}$ is close to 1. Thus the resonant amplification in $P_{\mu\mu}$ occurs within a narrow range of pathlengths for all the allowed values of θ_{13} , thus making $P_{\mu\mu}$ a suitable observable to study it. We obtain this pathlength to be about 7000 km by substituting the mantle density of earth $\rho = 4.5 \text{ gm/cc}$ and $p = 1$ in Eq.(3). From a numerical study we have identified the energy range 5 - 10 GeV and the pathlength range 6000 - 9000 km to be suitable for studying resonant amplification of matter effects in $P_{\mu\mu}$. In the case of $P_{\mu\tau}$, the pathlength for which matter effects cause the largest change is given by [40]⁴

$$[\rho L]_{\mu\tau}^{\max} \simeq \frac{(2p+1)}{2} \pi \cos 2\theta_{13} \times 10^4 \text{ km gm/cc}. \quad (4)$$

Here again the resonance amplification occurs for essentially the same pathlength for all allowed values of θ_{13} . Setting $p = 1$, in Eq.(4), we get this pathlength to be about 9700 km⁵. A numerical study shows that the energy range 4 - 8 GeV and pathlength range 8000 - 10500 GeV is suitable to study matter effects in $P_{\mu\mu}$ induced by large matter-induced changes in $P_{\mu\tau}$.

For the long pathlengths under consideration here, we need to explicitly take into account the varying density profile of the earth. We use the density profile given in Preliminary Reference Earth Model (PREM) [41]. In Figure 1 we plot $P_{\mu\mu}$ as a function of energy for four different pathlengths in the range 6000 to 9000 km. In all of these four cases, the most significant matter effects occur in the energy range 5 - 10 GeV. In Figure 2 we plot $P_{\mu\mu}$ as a function of energy for the two pathlengths 9700 km and 10500 km. In both these cases the most significant matter effects occur in the energy range 4 - 6 GeV. The curves Figure 1 and Figure 2 have been obtained by numerically solving the full three flavour neutrino propagation equation through earth matter. In obtaining these curves we have used the following values for neutrino parameters: $|\Delta_{31}| = 0.002 \text{ eV}^2$, $\Delta_{21} = 8.3 \times 10^{-5} \text{ eV}^2$, $\sin^2 \theta_{12} = 0.28$, $\sin^2 \theta_{23} = 0.5$ and $\sin^2 2\theta_{13} = 0.1$. For each of the six pathlengths, the muon neutrino survival probability $P_{\mu\mu}$ is calculated in vacuum and in matter for both the signs of Δ_{31} .

The following comments are in order :

- For negative Δ_{31} (or inverted hierarchy), there is no discernible difference between vacuum and matter survival probabilities.

⁴Note that in [40] $\cos 2\theta_{13}$ is misprinted as $\cos^2 \theta_{13}$. hep-ph/0408361, v3 has the correct expression.

⁵For $p = 0$, or the $\pi/2$ peak, the matter-induced change in $P_{\mu\tau}$ is seen to be small [28].

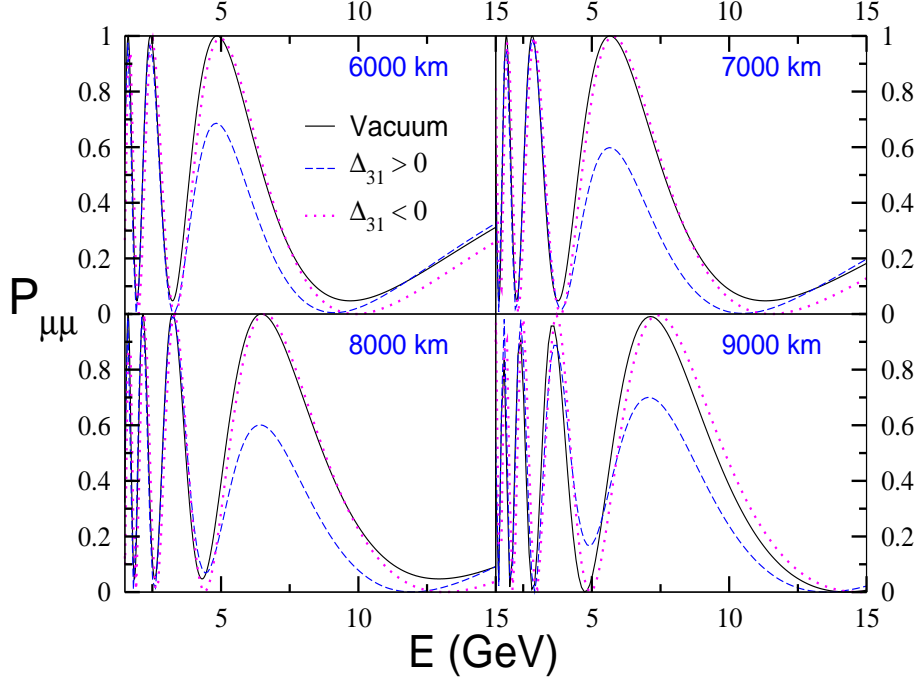


Figure 1: The muon survival probability $P_{\mu\mu}$ in matter plotted as a function of E (GeV) for four pathlengths, $L = 6000, 7000, 8000$ and 9000 km and for the two signs of Δ_{31} . The values of parameters used are $\sin^2 \theta_{12} = 0.28$, $\sin^2 \theta_{23} = 0.5$, $\sin^2 2\theta_{13} = 0.1$, $|\Delta_{31}| = 2 \times 10^{-3} \text{ eV}^2$ and $\Delta_{21} = 8.3 \times 10^{-5} \text{ eV}^2$. The survival probability in vacuum is also shown for comparison.

- For positive Δ_{31} (or normal hierarchy), the value of $P_{\mu\mu}$ in matter shown in Figure 1 suffers a drop with respect to its vacuum value in the energy range 5 - 10 GeV. Whereas, the $P_{\mu\mu}$ shown in Figure 2 undergoes an increase in the energy range 4 - 7 GeV.
- For the pathlength range 6000 - 9000 km, the change in $P_{\mu\mu}$, due to matter effects, is dominated by change in $P_{\mu e}$. In the vicinity of the vacuum peak, matter $P_{\mu\mu}$ is smaller by about 40% compared to the vacuum value. Three fourths of this change occurs due to change in $P_{\mu e}$ and the rest is due to change in $P_{\mu\tau}$ [28]. This is illustrated in Figure 1.
- For pathlengths $\gtrsim 9000$ km the matter effect in $P_{\mu\tau}$ also becomes significant. For such pathlengths, there is a drop in $P_{\mu\tau}$ which is as high as 70%, in the energy range 4 - 6 GeV. This drop in $P_{\mu\tau}$ overcomes the rise in $P_{\mu e}$. Thus the net change in $P_{\mu\mu}$ is an increase of the matter value over its vacuum value [40, 28]. This is illustrated in Figure 2 for two pathlengths 9700 km and 10500 km.
- Beyond 10500 km the neutrinos start traversing the core and the mantle-core interference effects set in [42]. It was shown in [28] that at such pathlengths and energies relevant for atmospheric neutrinos the difference between the vacuum and matter event rates are not significant⁶. Hence we do not include such pathlengths in our analysis.

⁶In the energy range ~ 3 -6 GeV there is some difference between matter and vacuum rates due to mantle-

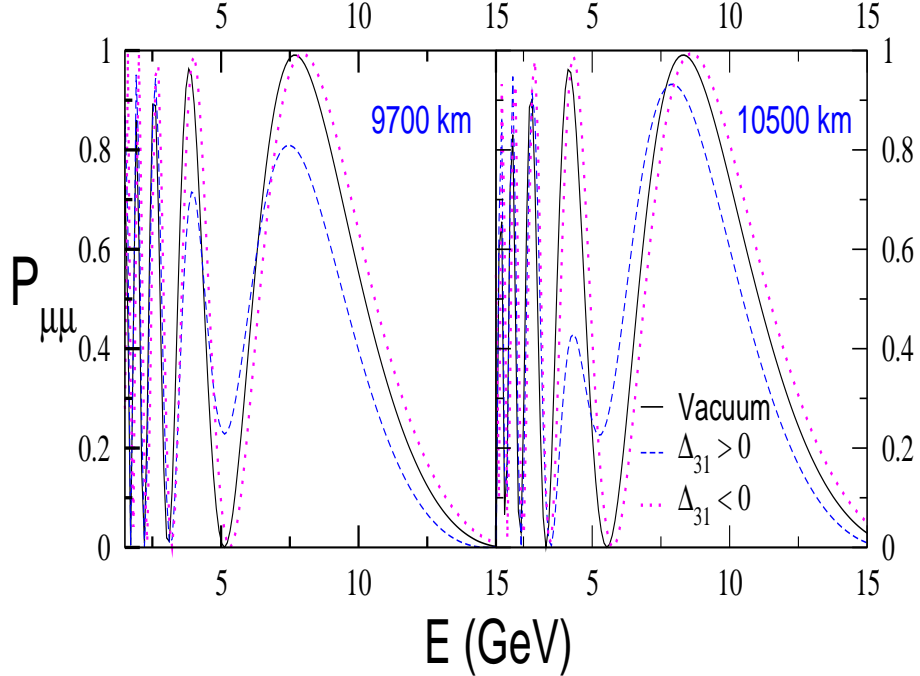


Figure 2: The muon survival probability $P_{\mu\mu}$ in matter plotted as a function of E (GeV) for two pathlengths, $L = 9700$ and 10500 km and for the two signs of Δ_{31} . The values of parameters used are $\sin^2 \theta_{12} = 0.28$, $\sin^2 \theta_{23} = 0.5$, $\sin^2 2\theta_{13} = 0.1$, $|\Delta_{31}| = 2 \times 10^{-3} \text{ eV}^2$ and $\Delta_{21} = 8.3 \times 10^{-5} \text{ eV}^2$. The survival probability in vacuum is also shown for comparison.

- In the case of muon antineutrinos, $P_{\bar{\mu}\bar{\mu}}$ is essentially unchanged for the case of positive Δ_{31} . It will experience resonance enhanced suppression for the case of negative Δ_{31} , which again can be as large as 40% for pathlengths in the range 6000 - 9000 km.

It is clear from Figure 1 and Figure 2 that matter effects in $P_{\mu\mu}$ can be large, and a high statistics measurement of the muon survival rate in the energy and pathlength ranges indicated can be used to detect their presence as well as pin down the mass hierarchy. Atmospheric neutrinos passing through earth's mantle have the relevant pathlengths and possess energies in the desired range and thus are well-suited for this purpose.

In general, these effects are sensitive to $\sin^2 \theta_{13}$, as mentioned earlier. This sensitivity, along with other aspects, was recently studied for a charge discriminating detector in [26, 27, 28]. In [28], it was emphasized that a conclusive and statistically significant determination of the hierarchy and associated matter effects in such a detector requires a careful selection of pathlength and energy range. It was shown that a 4σ signal for matter effects is possible with an exposure of 1000 Ktyr in a typical iron calorimeter detector [44, 45] when muon events in the energy range 5 - 10 GeV and the pathlength range 6000 - 9700 km are considered. Wider ranges of energies and pathlengths result in an averaging out of the signal for matter effects [28]. In what follows, we study the sensitivity of the $\nu_\mu + \bar{\nu}_\mu$ survival rate to the hierarchy core interference effects [43].

and to matter effects for a megaton size water Čerenkov detector.

3 Numerical results for water Čerenkov detectors

In order to determine the type of neutrino mass hierarchy, we exploit the muon neutrino and antineutrino disappearance channels. For a normal hierarchy (NH), the resonant amplification of matter effects occurs only for neutrinos, while for an inverted hierarchy (IH) it occurs only for anti-neutrinos. From Figure 1 and Figure 2 we see that, for a NH, the μ^- rate undergoes a change due to matter effects but the μ^+ rate is essentially the same as the vacuum oscillation rate. In the case of an IH, the situation is reversed. Here we have to make a distinction between two different kinematic choices:

1. E = 5 - 10 GeV and L = 6000 - 9000 km: In this energy and pathlength ranges the decrease in $P_{\mu\mu}$ is induced mainly by the increase in $P_{\mu e}$. For a NH, matter effects suppress the μ^- event rates by a large fraction (about 25%) compared to their vacuum oscillation rates whereas the μ^+ event rates will be essentially the same as their vacuum oscillation values. For an IH, the μ^- rates are equal to their vacuum rates and the μ^+ rates undergo significant suppression. These results follow from the plots of $P_{\mu\mu}$ shown in Figure 1.
2. E = 4 - 6 GeV and L = 9000 - 10500 km: In this energy and pathlength ranges $P_{\mu\mu}$ increases due to a sharp fall in $P_{\mu\tau}$. For a NH, matter effects increase the μ^- rates compared to their vacuum oscillation rates whereas, once again, the μ^+ rates are unaffected. For an IH, the situation is reversed. Once again, these results are apparent in the plots shown in Figure 2.

In a charge discriminating detector, which detects μ^- and μ^+ rates individually, a comparison of the μ^- event rate with that expected from vacuum oscillations is enough to determine $\text{sign}(\Delta_{31})$, whether the signal is measured in the ranges 1 or in ranges 2 [28]. Water Čerenkov detectors are insensitive to the sign of the leptonic charge on an event-by-event basis. Therefore, we sum over the rates of μ^- and μ^+ events and label the sum as ‘muon events’. Hence, for both normal and inverted hierarchies, the total muon event rate due to matter oscillations will be less(more) than the corresponding rate in the case of vacuum oscillations in the case of ranges 1(2).

While the summation of events over muons and anti-muons dilutes the sensitivity of water Čerenkov detectors to matter effects compared to charge discriminating detectors, the proposed megaton mass overrides this disadvantage and provides the statistics necessary for a determination of the hierarchy. It is also to be noted that the μ^- event rates are 2 to 3 times larger than those of the μ^+ rates due to the larger $\nu_\mu - N$ cross section. Thus a larger change in the total muon event rate and a statistically stronger signal of matter resonance effects is envisioned in the case of a NH than in the case of an IH in both types of detectors.

The total number of muon (or anti-muon) charged current (CC) events can be obtained by folding the relevant CC cross section with the survival probability, the incident neutrino flux, the efficiency for detection, the detector mass and the exposure time. In our calculations,

the cross sections for $\nu_\mu - N$ and $\bar{\nu}_\mu - N$ interactions have been taken from [46]. The total CC cross section is sum of quasi-elastic, single meson production and deep inelastic cross sections.

Before describing our calculation and the results, we first state the assumptions we have made. We assume that the neutrino oscillation parameters $|\Delta_{31}|$ and θ_{23} will be determined to better than 10% accuracy by the long baseline experiments MINOS [48] and T2K [5] by the time megaton size water Čerenkov detectors are operative. In addition, we have assumed that similar precision will exist for the measured values of Δ_{21} and θ_{12} [1, 49], even though the dependence of our results on them is marginal. Based as they are on survival rates and large matter effects, our conclusions are also effectively independent of the CP violating phase δ_{CP} . Finally, for our method to yield results over running times of 3-4 years, $\sin^2 2\theta_{13}$ must be ≥ 0.05 .

For the first set of our calculations, we use the following values for all neutrino parameters known to be non-zero: $|\Delta_{31}| = 0.002 \text{ eV}^2$, $\Delta_{21} = 8.3 \times 10^{-5} \text{ eV}^2$, $\sin^2 \theta_{23} = 0.5$ and $\sin^2 \theta_{12} = 0.28$. We calculate the event rates for four different values of θ_{13} , i.e. $\sin^2 2\theta_{13} = 0.05, 0.1, 0.15, 0.2$. In a later set of calculations, we vary θ_{23} and $|\Delta_{31}|$ within the ranges allowed by SK atmospheric neutrino data and K2K results to gauge the dependence of our results on them.

To study the sensitivity of the megaton water Čerenkov detectors to the hierarchy, we compute the expected number of $\mu^- + \mu^+$ events in the following four cases:

- No oscillations, N_{Down} ,
- Vacuum oscillations, N_{vac} ,
- Matter oscillations with NH, N_{NH} and
- Matter oscillations with IH, N_{IH} .

If the difference between N_{NH} and N_{IH} is statistically significant, then $\text{sign}(\Delta_{31})$ can be assumed to established with this same significance. Thus

$$N_\sigma = \frac{|N_{\text{NH}} - N_{\text{IH}}|}{\sqrt{N_{\text{NH}}}} \quad (5)$$

gives the *sigma confidence level with which the expectation for NH differs from that for IH*.

We note that Eq.(5) tacitly assumes that atmospheric neutrino fluxes will be measured well enough in the next decade to allow use of the absolute event rates. However, if this is not the case, one can also use the *measured* number of downward going events, which have the same corresponding values of $|\cos \theta_{\text{zenith}}|$ as the upgoing events, as an estimate for the number of events in case of no oscillations. This is the reason why we have denoted these as N_{Down} above. In such a situation, we can usefully consider the ratios $R_{\text{NH}} = N_{\text{NH}}/N_{\text{Down}}$ and $R_{\text{IH}} = N_{\text{IH}}/N_{\text{Down}}$. The statistical significance of the difference between the ratios is then defined as

$$N_{\sigma_R} = \frac{|R_{\text{NH}} - R_{\text{IH}}|}{R_{\text{NH}} \sqrt{1/N_{\text{NH}} + 1/N_{\text{Down}}}}. \quad (6)$$

$\sin^2 2\theta_{13}$	N_{vac}	N_{NH}	N_{IH}	N_{σ}	R_{NH}	R_{IH}	$N_{\sigma_{\text{R}}}$
0.05	111	101	111	1 σ	0.56	0.62	0.8 σ
0.10	110	92	107	1.6 σ	0.52	0.6	1.2 σ
0.15	108	82	103	2.3 σ	0.46	0.58	2 σ
0.20	108	76	100	2.8 σ	0.43	0.56	2.2 σ

Table 1: Integrated muon event numbers for SK (337.5 Ktyr) for the energy range $E = 5 - 10$ GeV and pathlength range $L = 6000 - 9000$ km. The expected event numbers in the case of vacuum oscillations (N_{vac}) and matter oscillations for both NH (N_{NH}) and IH (N_{IH}) are calculated with $\sin^2 \theta_{23} = 0.5$, $|\Delta_{31}| = 0.002 \text{ eV}^2$, and various different values of θ_{13} . The number of downward events $N_{\text{Down}} = 178$ is used in calculating the ratios $R_{\text{NH}} = N_{\text{NH}}/N_{\text{Down}}$ and $R_{\text{IH}} = N_{\text{IH}}/N_{\text{Down}}$

Our first set of results is for SuperKamiokande (SK) for 15 years of running. Since the SK fiducial volume is 22.5 Kt, this gives us an exposure⁷ of 337.5 Ktyr. We use the Bartol fluxes from [50] and incorporate the SK cross sections, resolutions [46, 51] and efficiencies [52]. In calculating the number of events, we have integrated over the neutrino energy range = 5 - 10 GeV and pathlength range $L = 6000 - 9000$ km. For $\Delta_{31} = 0.002 \text{ eV}^2$, the resonance in earth's mantle occurs for energy of about 6.5 GeV. Since we are looking for resonant amplification of matter effects, we have chosen the energy range so that it encompasses this energy. We note that this choice is also dependant on the fact that $|\Delta_{31}| = 0.002 \text{ eV}^2$. For other values of $|\Delta_{31}|$, the appropriate energy range will be different. It was shown earlier that the pathlength for which the resonant matter effects are maximum is about 7000 km. In this calculation, we choose a range of pathlengths, 6000 - 9000 km, in order to utilize the enhancement associated with this value.

Table 1 gives our results for SK for an exposure time of 337.5 Ktyr. We find that, even for the largest allowed value of $\sin^2 2\theta_{13}$, the expectations for NH and IH differ by 2.8σ if we have reliable predictions for neutrino fluxes. If one needs to take ratios to cancel flux uncertainties, then the confidence level in the difference reduces to 2.2σ . These low confidence levels result from the small event rates of atmospheric neutrinos at high (*i.e* several GeV) energies. Since the observation of the resonant amplification of matter effects requires energies in the 4 – 10 GeV range, the larger exposures which are possible at planned megaton size detectors such as HyperKamiokande (HK) [6, 33] (higher by a factor of 6 to 20 compared to SK) are required to obtain a statistically significant signal. The proposed fiducial volume of HK is 545 Kt. Hence, with a running time of only 3.3 years, it will be possible to have a total exposure of 1.8 Mtyr, which is a factor **6** larger than what is possible at SK. In the calculation of the muon event rates for HK, we have used the efficiencies and resolutions of SK [52].

Figure 3 shows the L/E distribution of events for matter oscillations (for both a NH and an IH) by plotting the events versus $\text{Log}_{10}(L/E)$ for HK in the energy range from 5 - 10 GeV and pathlength range 6000 - 9000 km, with $\sin^2 2\theta_{13} = 0.1$. Assuming an L/E resolution similar to SK allows a division into five bins in $\text{Log}_{10}(L/E)$ for this L and E range [51]. The drop in N_{NH} relative to N_{IH} is evident in the third and fourth bins in this figure. In these

⁷In the latest SK paper [46], the exposure is 92 Ktyr corresponding to 1489 days live time from May 1996 to July 2001. Preliminary results for SK-II include a further 627 days live time [47].

$\sin^2 2\theta_{13}$	N_{vac}	N_{NH}	N_{IH}	N_{σ}	R_{NH}	R_{IH}	$N_{\sigma_{\text{R}}}$
0.05	593	537	596	2.5σ	0.56	0.63	2.3σ
0.10	588	490	571	3.7σ	0.52	0.6	2.8σ
0.15	578	439	552	5.4σ	0.46	0.58	4.5σ
0.20	576	406	533	6.3σ	0.43	0.56	5.1σ

Table 2: Integrated muon event numbers for HK (exposure of 1.8 Mtyr) for the energy range $E = 5 - 10$ GeV and pathlength range $L = 6000 - 9000$ km. The expected event numbers in the case of vacuum oscillations (N_{vac}) and matter oscillations for both NH (N_{NH}) and IH (N_{IH}) are calculated with $\sin^2 \theta_{23} = 0.5$, $|\Delta_{31}| = 0.002 \text{ eV}^2$, and various different values of θ_{13} . The number of downward events $N_{\text{Down}} = 951$ is used in calculating the ratios $R_{\text{NH}} = N_{\text{NH}}/N_{\text{Down}}$ and $R_{\text{IH}} = N_{\text{IH}}/N_{\text{Down}}$

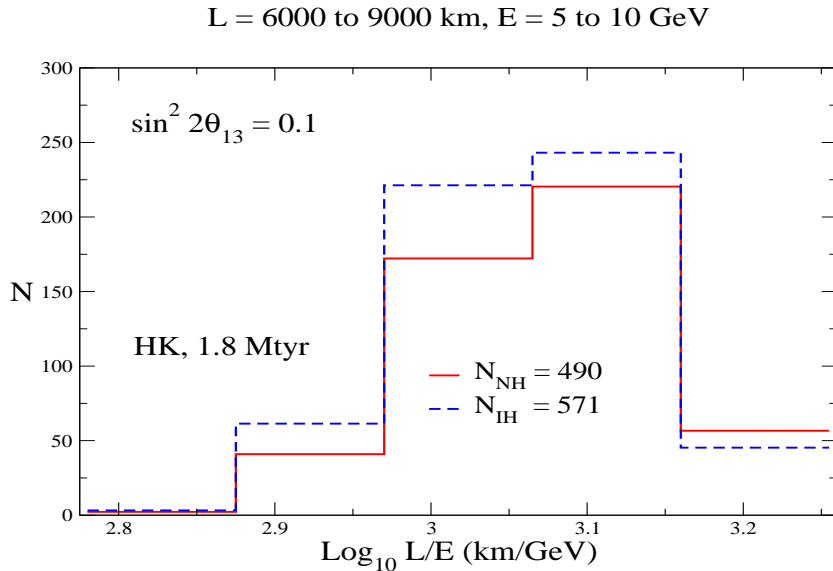


Figure 3: Muon ($\nu_{\mu} + \bar{\nu}_{\mu}$) event distribution for HK(1.8 Mtyr) of matter oscillations for NH and for IH plotted vs $\text{Log}_{10}(L/E)$ for the E and L range $E = 5-10$ GeV, $L = 6000-9000$ km. The values of parameters used are $\sin^2 \theta_{12} = 0.28$, $\sin^2 \theta_{23} = 0.5$, $\sin^2 2\theta_{13} = 0.1$, $|\Delta_{31}| = 2 \times 10^{-3} \text{ eV}^2$ and $|\Delta_{21}| = 8.3 \times 10^{-5} \text{ eV}^2$.

energy and zenith angle ranges the change in $P_{\mu\mu}$ is predominantly due to the matter effect in $P_{\mu e}$. In Table 2 we present the N_{σ} values calculated using Eq.5. We first sum over the events of all the 5 bins shown in Figure 3 and then compute N_{σ} . For $\sin^2 2\theta_{13} = 0.1$ the sensitivity is 3.7σ . If instead we consider only the 3rd and 4th bins of Figure 3 and sum the number of events in these two bins then we get $N_{\text{NH}} = 400$ and $N_{\text{IH}} = 475$, which correspond to a sensitivity of 3.8σ . Making a narrow choice of bins in (L/E) does not improve the sensitivity as the effect is distributed over a larger L and E range. However, we will show later that for the L and E ranges for which the matter effects in $P_{\mu\mu}$ arise dominantly from $P_{\mu\tau}$, binning in (L/E) leads to a great improvement in the sensitivity to mass hierarchy.

As shown in Table 2, we obtain a $\gtrsim 3.7\sigma$ difference between N_{NH} and N_{IH} for $\sin^2 2\theta_{13} \gtrsim 0.1$, for an exposure of 1.8 Mtyr. Even when we have to take ratios with respect to downward

$\sin^2 \theta_{23}$	N_{vac}	N_{NH}	N_{IH}	N_σ	R_{NH}	R_{IH}	$N_{\sigma_{\text{R}}}$
0.4	599	524	596	3.1σ	0.55	0.63	2.8σ
0.5	588	490	571	3.7σ	0.52	0.6	2.8σ
0.6	596	475	576	4.6σ	0.5	0.6	3.6σ

Table 3: Integrated muon event numbers for HK (exposure of 1.8 Mtyr) for the energy range $E = 5 - 10$ GeV and pathlength range $L = 6000 - 9000$ km. The expected event numbers in the case of vacuum oscillations (N_{vac}) and matter oscillations for both NH (N_{NH}) and IH (N_{IH}) are calculated with $\sin^2 2\theta_{13} = 0.1$, $|\Delta_{31}| = 0.002 \text{ eV}^2$, and various different values of θ_{23} . The number of downward events $N_{\text{Down}} = 951$ is used in calculating the ratios $R_{\text{NH}} = N_{\text{NH}}/N_{\text{Down}}$ and $R_{\text{IH}} = N_{\text{IH}}/N_{\text{Down}}$.

events, this difference is close to 3σ . With an exposure of about 3 Mtyr (which corresponds to a running time of about 6 years), one can obtain a 3σ difference between N_{NH} and N_{IH} , for $\sin^2 2\theta_{13} \simeq 0.05$.

Next, we check how N_σ and $N_{\sigma_{\text{R}}}$ change with variation of neutrino parameters. We first illustrate the dependence on θ_{23} . For this purpose we fix $\sin^2 2\theta_{13} = 0.1$ and consider three different values of $\sin^2 \theta_{23} = 0.4, 0.5$ and 0.6 . The sensitivities for these values of θ_{23} are shown in Table 3 for HK exposure of 1.8 Mtyr. The energy range (5 - 10 GeV) and the pathlength range (6000 - 9000 km) remain the same because $|\Delta_{31}|$ is unchanged. We note from Table 3 that the sensitivities are better for $\sin^2 \theta_{23} = 0.6$ and worse for $\sin^2 \theta_{23} = 0.4$ compared to the $\sin^2 \theta_{23} = 0.5$ case. The reason for this is simple. As mentioned earlier, the matter effects in $P_{\mu\mu}$ arise mostly due to the matter effects in $P_{\mu e}$. The matter term in $P_{\mu e}$ is proportional to $\sin^2 \theta_{23}$. Therefore, for a larger value of $\sin^2 \theta_{23}$ we get a larger change in $P_{\mu\mu}$ due to matter effects and hence there is a larger difference between the expected rates for NH and IH cases.

We next study the change in the sensitivities with variation in $|\Delta_{31}|$. We fix $\sin^2 \theta_{23} = 0.5$, $\sin^2 2\theta_{13} = 0.1$ and consider three different values of $|\Delta_{31}| = 0.001, 0.002$ and 0.003 eV^2 and calculate the muon event rates for HK exposure of 1.8 Mtyr by integrating over appropriate energy and pathlength ranges. From Eq.(1), we note that the resonance occurs at different energies for different values of $|\Delta_{31}|$. For 0.003 eV^2 , it occurs at 9.5 GeV. So we choose the energy range of integration to be 7 – 12 GeV. For 0.001 eV^2 , the resonance occurs at 3.2 GeV, so we choose the energy range to be 2 – 5 GeV. But the pathlength range remains unchanged at 6000 - 9000 km. This is because Eq.(3) shows that the expression for the pathlength for resonant amplification of matter effects is independent of Δ_{31} . The event numbers and the corresponding sensitivities for this case are given in Table 4. We note that in general one expects a fall the in sensitivity for higher values of $|\Delta_{31}|$ due to the higher resonance energies (and consequently lower number of total events) ⁸.

It was shown in references [40, 28] that for certain ranges of L and E , $P_{\mu\mu}$ is larger compared to its vacuum value, due to a sharp fall (by as much as 70%) in $P_{\mu\tau}$. For $|\Delta_{31}| = 0.002 \text{ eV}^2$, this occurs in the energy range 4 - 6 GeV and pathlength range 8000 - 10500 km. In Figure 4 the total muon event rates are computed and plotted as function of L/E for values

⁸That this is not the case for $|\Delta_{31}| = 0.002$ compared to $|\Delta_{31}| = 0.001$ in our table is attributable to the fact that the energy range for the best fit value of $|\Delta_{31}| = 0.002$ has been optimized, while that for the other two values has been chosen merely for illustrative purposes.

Δ_{31}	E_{res}	E Range	N_{Down}	N_{vac}	N_{NH}	N_{IH}	N_{σ}	R_{NH}	R_{IH}	$N_{\sigma_{\text{R}}}$
0.001	3.2 GeV	2 - 5 GeV	2080	1164	1020	1125	3.3 σ	0.49	0.54	2.7 σ
0.002	6.5 GeV	5 - 10 GeV	951	588	490	571	3.7 σ	0.52	0.6	2.8 σ
0.003	9.5 GeV	7 - 12 GeV	598	434	356	398	2.2 σ	0.59	0.67	1.8 σ

Table 4: Muon event numbers for HK for an exposure of 1.8 Mtyr for different values of $|\Delta_{31}|$. The pathlength range, $L = 6000 - 9000$ km, is the same for all three cases but the energy ranges are different because the resonance energies are different. The expected event numbers in the case of vacuum oscillations (N_{vac}) and matter oscillations for both NH (N_{NH}) and IH (N_{IH}) are calculated with $\sin^2 \theta_{23} = 0.5$ and $\sin^2 2\theta_{13} = 0.1$. Because of different energy ranges, the number of downward events in each case is different and are listed in table. They are used in calculating the ratios $R_{\text{NH}} = N_{\text{NH}}/N_{\text{Down}}$ and $R_{\text{IH}} = N_{\text{IH}}/N_{\text{Down}}$

$\sin^2 2\theta_{13}$	N_{vac}	N_{NH}	N_{IH}	N_{σ}	R_{NH}	R_{IH}	$N_{\sigma_{\text{R}}}$
0.05	40	68	46	2.6 σ	0.21	0.14	2.5 σ
0.10	41	96	58	3.9 σ	0.3	0.18	3.4σ
0.15	49	130	74	4.9 σ	0.4	0.23	4.1 σ
0.20	50	158	86	5.7 σ	0.49	0.26	4.8 σ

Table 5: Integrated muon event numbers for HK (exposure of 1.8 Mtyr). The events selected are those in the energy range $E = 4 - 8$ GeV and pathlength range $L = 8000 - 10500$ km, with $\text{Log}_{10}(L/E) = 3.2 - 3.3$. The expected event numbers in the case of vacuum oscillations (N_{vac}) and matter oscillations for both NH (N_{NH}) and IH (N_{IH}) are calculated with $\sin^2 \theta_{23} = 0.5$, $|\Delta_{31}| = 0.002$ eV², and various different values of θ_{13} . The number of downward events $N_{\text{Down}} = 325$ is used in calculating the ratios $R_{\text{NH}} = N_{\text{NH}}/N_{\text{Down}}$ and $R_{\text{IH}} = N_{\text{IH}}/N_{\text{Down}}$

of $\text{Log}_{10}(L/E)$ in the range 3.0 - 3.4. If we assume **SK** resolutions, this range can be divided into four bins. We see that for the bin with $\text{Log}_{10}(L/E) = 3.2 - 3.3$ the change due to the sign of Δ_{31} is particularly pronounced. Note also that, as mentioned above, unlike the previous ranges, here *the expected number of muon events for the case of NH is larger than that for the case of IH*. This phenomenon, however, occurs only for narrow ranges in energy and pathlength and hence one needs a detector with good L/E resolution to observe it. Given a detector with such resolution however, the difference in the expected muon rates in the bin with $\text{Log}_{10}(L/E) = 3.2 - 3.3$ is an excellent indicator of the neutrino mass hierarchy. From the event numbers given in Table 5, we see that the difference in this bin corresponds to a **4 σ** signal for $\sin^2 2\theta_{13} = 0.1$ with an exposure of just 1.8 Mtyr in HK. If we sum the events in the two bins with $\text{Log}_{10}(L/E) = 3.1 - 3.2$ and $3.2 - 3.3$, the difference between the expectations for NH and IH corresponds to a sensitivity of **3 σ** .

Table 5 also gives the number of events in matter ($\Delta_{31} > 0$) and the values of σ sensitivity for this $\text{Log}_{10}(L/E)$ bin for three values of θ_{13} . This shows a higher sensitivity as compared to Table 2 and more than 2.5 σ sensitivity can be achieved for $\sin^2 2\theta_{13} = 0.05$ with the exposure considered here.

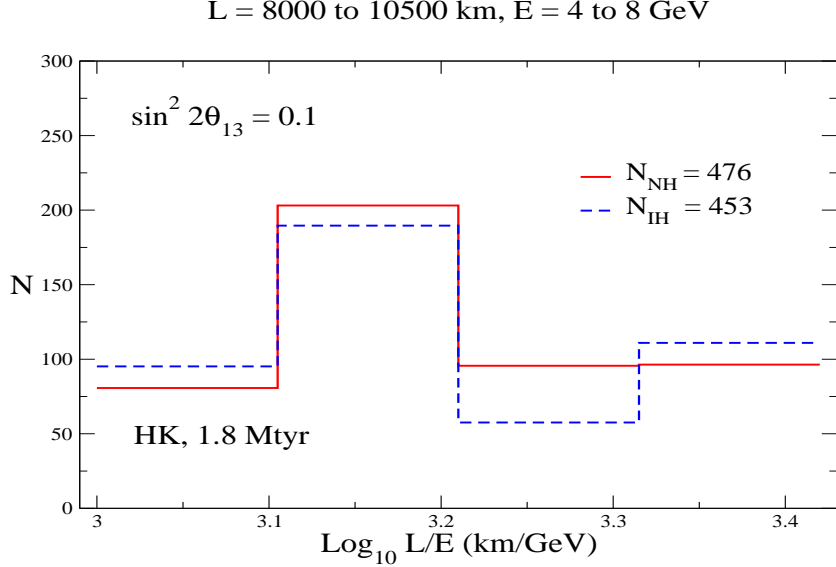


Figure 4: Muon ($\nu_\mu + \bar{\nu}_\mu$) event distribution for HK(1.8 Mtyr) in matter and in vacuum plotted vs $\text{Log}_{10}(L/E)$ for the E and L range E = 4-8 GeV, L = 8000-10500 km. The values of parameters used are $\sin^2 \theta_{12} = 0.28$, $\sin^2 \theta_{23} = 0.5$, $\sin^2 2\theta_{13} = 0.1$, $|\Delta_{31}| = 2 \times 10^{-3} \text{ eV}^2$ and $|\Delta_{21}| = 8.3 \times 10^{-5} \text{ eV}^2$.

4 Conclusions

- The neutrino mass hierarchy, presently unknown, is a powerful discriminator among various classes of unification theories. We have shown that the total muon ($\nu_\mu + \bar{\nu}_\mu$) survival rate in atmospheric events can provide a novel and useful method of determining the hierarchy in megaton water Čerenkov detectors⁹.
- The rates for both normal and inverted hierarchies differ from the vacuum rate and from each other due to large matter sensitive variations not only in $P_{\mu e}$ but also in $P_{\mu\tau}$. We have identified energy and pathlength ranges where these effects can be fruitfully observed in a statistically significant manner for running times of $\sim 3-4$ years for values of $\sin^2 \theta_{13} \geq 0.05$.
- We have calculated the σ sensitivities for normal and inverted hierarchies via differences in absolute events as well as differences in event ratios (to eliminate uncertainties in the atmospheric flux) for various choices of the neutrino parameters. We find that the energy ranges 5–10 GeV and 4–8 GeV, when combined with the length ranges 6000–9000 km and 8000–10500 km respectively¹⁰, allow for a statistically significant determination of the hierarchy. The first (L,E) range combination allows us to probe the $P_{\mu e}$ -induced

⁹Even though we have presented the results for HK, our conclusions should remain valid for similar detectors such as UNO [33] or the one proposed in Frejus tunnel [34] in Europe.

¹⁰In the latter case, as discussed in the context of Figure 4, the effect is apparent in the L/E bin specified by $\text{Log}_{10}(L/E) = 3.2 - 3.3$.

matter effects in $P_{\mu\mu}$, while the second combination provides a way of detecting the $P_{\mu\tau}$ effects in $P_{\mu\mu}$.

- Finally, we have also studied the dependence of our results on the uncertainties in the presently known values of $\sin^2 \theta_{23}$ and $|\Delta_{31}|$.

Acknowledgements

The authors thank T. Kajita for useful communications and S. Choubey for useful discussions regarding the statistical sensitivity for Normal and Inverted hierarchy. P.M. wants to thank the Weizmann Institute of Science, Israel for hospitality. RG would like to thank the Stanford Linear Accelerator Center (SLAC) and the Institute for Nuclear Theory (INT) at the University of Washington for hospitality while this work was in progress.

References

- [1] For a recent review, see S. Goswami, talk at *XXIst International Symposium on Lepton-Photon Interactions at High Energy (Lepton-Photon 2005)*, Uppsala, Sweden, 30 Jun - 5 July 2005; A. Bandyopadhyay, S. Choubey, and S. Goswami, Nucl. Phys. Proc. Suppl. **143**, 121-128 (2005); hep-ph/0409224 and references therein.
- [2] For a recent review, see R.N. Mohapatra, hep-ph 0412379; and references therein.
- [3] C. H. Albright, Phys. Lett. B **599**, 285 (2004).
- [4] A. de Gouvea, J. Jenkins and B. Kayser, hep-ph/0503079; H. Nunokawa, S. Parke and R. Z. Funchal, hep-ph/0503283.
- [5] Y. Hayato, talk at *XXIst International Conference on Neutrino Physics and Astrophysics (Neutrino-2004)*, Paris, June 14-19, 2004, see <http://neutrino2004.in2p3.fr/> ; see <http://neutrino.kek.jp/jhfnu~>.
- [6] Y. Itow *et al.*, Nucl. Phys. B, Proc. Suppl. **111**, 146 (2001), The JHF-Kamioka neutrino project, hep-ex/0106019.
- [7] NOVA collaboration, I. Ambats *et al.*, FERMILAB-PROPOSAL-0929, see <http://library.fnal.gov/archive/test-proposal/0000/fermilab-proposal-0929.shtml/> ; NOVA collaboration, D. Ayres *et al.*, hep-ex/0210005, <http://www-off-axis.fnal.gov/> ; A. Weber, Eur. Phys. J C **33**, s843-s845 (2004); M. Messier, talk at *XXIst International Conference on Neutrino Physics and Astrophysics (Neutrino-2004)*, Paris, June 14-19, 2004, see <http://neutrino2004.in2p3.fr/>.
- [8] P. Huber, *et al.*, Phys. Rev. D **70**, 073014 (2004).

- [9] H. Minakata, H. Nunokawa and S. J. Parke, Phys. Rev. D **68**, 013010 (2003).
- [10] O. Mena and S. J. Parke, Phys. Rev. D **70**, 093011 (2004).
- [11] O. Mena and S. Parke, hep-ph/0505202.
- [12] J. Burguet-Castell *et al.*, Nucl. Phys. B **695**, 217 (2004).
- [13] V. D. Barger *et al.*, Phys. Lett. B **485**, 379 (2000).
- [14] See *for e.g.*, V. Barger, D. Marfatia and K. Whisnant, Phys. Rev. D **65**, 073023 (2002); H. Minakata, H. Nunokawa and S. J. Parke, Phys. Rev. D **66**, 093012 (2002).
- [15] V. Barger, D. Marfatia and K. Whisnant, Phys. Lett. B **560**, 75 (2003).
- [16] J. Burguet-Castell *et al.*, Nucl. Phys. B **646**, 301 (2002).
- [17] Y. F. Wang *et al.*, [VLBL Study Group H2B-4], Phys. Rev. D **65**, 073021 (2002).
- [18] K. Whisnant, J. M. Yang and B. L. Young, Phys. Rev. D **67**, 013004 (2003).
- [19] P. Huber, M. Lindner, T. Schwetz and W. Winter, Nucl. Phys. B **665**, 487 (2003).
- [20] A. Donini *et al.*, Nucl. Phys. B **710**, 402 (2005).
- [21] M. Ishitsuka *et al.*, hep-ph/0504026.
- [22] O. Mena Requejo, S. Palomares-Ruiz and S. Pascoli, hep-ph/0504015.
- [23] P. Huber and W. Winter, Phys. Rev. D **68**, 037301 (2003).
- [24] A. Asratyan *et al.*, hep-ex/0303023.
- [25] S. K. Agarwalla, A. Raychaudhuri and A. Samanta, hep-ph/0505015.
- [26] S. Palomares-Ruiz and S. T. Petcov, Nucl. Phys. B **712**, 392 (2005).
- [27] D. Indumathi and M. V. N. Murthy, Phys. Rev. D **71**, 013001 (2005).
- [28] R. Gandhi *et al.*, hep-ph/0411252.
- [29] See *for instance*, P. Huber, M. Maltoni and T. Schwetz, Phys. Rev. D **71**, 053006 (2005); J. Bernabeu, S. Palomares-Ruiz and S. T. Petcov, Nucl. Phys. B **669**, 255 (2003), and references therein.
- [30] See *for e.g.*, C. Lunardini and A. Y. Smirnov, JCAP **0306**, 009 (2003); C. Lunardini and A. Y. Smirnov, Nucl. Phys. B **616**, 307 (2001); A. S. Dighe, M. T. Keil and G. G. Raffelt, JCAP **0306**, 006 (2003); A. Bandyopadhyay *et al.*, hep-ph/0312315.

- [31] See *for e.g.*, S. Pascoli, S. T. Petcov and W. Rodejohann, Phys. Lett. B **558**, 141 (2003); S. Pascoli, S. T. Petcov and T. Schwetz, hep-ph/0505226; S. Choubey and W. Rodejohann, hep-ph/0506102 and references therein.
- [32] A. de Gouvea and J. Jenkins, hep-ph/0507021.
- [33] C. K. Jung, hep-ex/0005046, Published in *Stony Brook 1999, Next generation nucleon decay and neutrino detector, 29-34 (1999)*;
The UNO whitepaper, ‘Physics Potential and Feasibility of UNO’, SBHEP01-3 (2001), available at <http://ale.physics.sunysb.edu/uno/>.
- [34] L. Mosca, talk at ‘Physics with a Multi-MW Proton Source’, CERN, Geneva, 25–27 May 2004, available at <http://physicsatmwatt.web.cern.ch/physicsatmwatt/>.
- [35] T. Kajita, talk at *The 5th workshop on Neutrino Oscillations and their Origin*, see <http://www-sk.icrr.u-tokyo.ac.jp/noon2004/>.
- [36] L. Wolfenstein, Phys. Rev. D **17**, 2369 (1978); *ibid* D **20**, 2634 (1979).
- [37] CHOOZ Collaboration: M. Apollonio *et al.*, Eur. Phys. J. C **27**, 331 (2003);
Phys. Lett. B **420**, 397 (1998);
Phys. Lett. B **466**, 415 (1999);
M. Narayan, G. Rajasekaran and S. Uma Sankar, Phys. Rev. D **58** 031301 (1998).
- [38] S. Mikheyev and A. Yu. Smirnov, Nuovo Cimento **9C**, 17 (1986);
H. Bethe, Phys. Rev. Lett. **56**, 1305 (1986).
- [39] See *e.g.*, I. Mocioiu and R. Shrock, Phys. Rev. D **62**, 053017 (2000);
V. Barger *et al.*, *ibid.* **62**, 013004 (2000);
ibid. Phys. Lett. B **485**, 379 (2000);
M. Freund, M. Lindner, S. T. Petcov, A. Romanino, Nucl. Phys. B **578**, 27 (2000);
M. Freund, P. Huber, M. Lindner, Nucl. Phys. B **585**, 105 (2000);
M. Freund, M. Lindner, S. T. Petcov, A. Romanino, Nucl. Instrum. Meth **A451**, 18 (2000);
M. Freund, Phys. Rev. D **64**, 053003 (2001);
M. C. Banuls, G. Barenboim and J. Bernabeu, Phys. Lett. B **513**, 391 (2001);
E. K. Akhmedov *et al.*, JHEP **0404**, 078 (2004) and references therein.
- [40] R. Gandhi *et al.*, Phys. Rev. Lett. **94**, 051801 (2005) [hep-ph/0408361].
- [41] A. M. Dziewonski and D. L. Anderson, Phys. Earth Planet Int. **25** 297(1981); See http://solid_earth.ou.edu/prem.html;
We use the parameterization given in R. Gandhi et al., Astropart. Phys. **5**, 81 (1996).
- [42] S. T. Petcov, Phys. Lett. B **434**, 321 (1998);
E. K. Akhmedov *et al.*, Nucl. Phys. B **542**, 3 (1999);
M. Chizhov, M. Maris, S. T. Petcov, hep-ph/9810501;
M. V. Chizhov and S. T. Petcov, Phys. Rev. D **63**, 073003 (2001) ;
J. Bernabeu *et al.*, Phys. Lett. B **531**, 90 (2002).

- [43] S. T. Petcov, Private Communication.
- [44] MONOLITH collaboration, N. Y. Agafonova *et al.*, LNGS-P26-2000; <http://castore.mi.infn.it/~monolith/>.
- [45] INO collaboration, See <http://www.imsc.res.in/~ino> for INO Interim Report on feasibility studies and a collection of related papers and talks.
- [46] SUPER-KAMIOKANDE collaboration, Y. Ashie *et al.* Phys. Rev. Lett. **93**, 101801 (2004).
- [47] Y. Suzuki, talk at *XXIIst International Symposium on Lepton-Photon Interactions at High Energy (Lepton-Photon 2005)*, Uppsala, Sweden, 30 Jun - 5 July 2005.
- [48] M.A. Thompson, Nucl. Phys. Proc. Suppl. 143, 249-256, 2005, and references therein.
- [49] See A. Bandyopadhyay, S. Choubey, S. Goswami and S. T. Petcov, hep-ph/0410283.
- [50] V. Agrawal *et al.*, Phys. Rev. D **53**, 1314 (1996).
- [51] Y. Ashie *et al.*, hep-ex/0404034.
- [52] T. Kajita, Private Communication.
- [53] M. Maltoni *et al.*, New J. Phys. **6**, 122 (2004);
A. Bandyopadhyay *et al.*, Phys. Lett. B **608**, 115 (2005);
S. Goswami and A. Y. Smirnov, hep-ph/0411359.
- [54] A. Strumia and F. Vissani, hep-ph/0503246.